Conical Refraction in Second-Harmonic Generation*

H. SHIH AND N. BLOEMBERGEN
Division of Engineering and Applied Physics, Harvard University, Cambridge, Massachusetts 02139
(Received 28 June 1968; revised manuscript received 5 May 1969)

The second-harmonic generation in an optically nonlinear biaxial crystal is discussed, when the fundamental laser beam propagates along the direction of an optical axis for the harmonic wave. It is shown that in the case of phase mismatch, the harmonic radiation will be emitted in a cone mantle, which is the nonlinear analog of internal conical refraction. In the case of momentum matching along the optical axis, a more complex intensity distribution results which fills the entire apex angle of the cone.

I. INTRODUCTION

THE parametric generation of light in uniaxial crystals has been the subject of extensive investigations.[1–4] When a homogeneous plane wave of infinite cross section with a wave vector $\mathbf{k}_L$ propagates in a nonlinear piezoelectric crystal, it creates a harmonic polarization with wave vector $2\mathbf{k}_L$. The harmonic field inside the crystal is generally described by the superposition of two harmonic waves. One corresponds to the solution of the inhomogeneous wave equation and has a wave vector $\mathbf{K}=2\mathbf{k}_L$. The other corresponds to the free wave with wave vector $\mathbf{k}(2\omega)$. The direction of this wave vector is fixed by the condition that it has the same tangential component along the boundary of the crystal as $2\mathbf{k}_L$. The momentum mismatch is described by

$$\Delta\mathbf{k}=2\mathbf{k}_L(\omega)-\mathbf{k}(2\omega)=(\pi/l_{\mathrm{coh}})\hat{z}, \tag{1}$$

where $\hat{z}$ is unit vector normal to the boundary. The amplitudes of the two waves are determined by the continuity of the transverse components of $\mathbf{E}$ and $\mathbf{H}$ at the boundary. In order to avoid unnecessary complications, we may for the purposes of the present paper put the reflected harmonic amplitude equal to zero, and obtain to a good approximation

$$|E_{\mathrm{inh}}|=|E_{\mathrm{hom}}|\cong 2\pi(2\omega/cn)P^{\mathrm{NL}}/(\Delta k). \tag{2}$$

More precise and complete expressions will be developed in Secs. II and III. For a laser beam of finite cross section one has a distribution over a small range of transverse components of the wave vector $\mathbf{K}_1$, and the resulting harmonic field must be obtained by an integration of $\mathbf{K}_1$ for both the homogeneous and the inhomogeneous solution. If the harmonic polarization direction created by a fundamental wave with ordinary polarization corresponds to the extraordinary ray in the uniaxial crystal, the group velocity of such a wave packet will make an angle ρ with the wave vector.[5] The direction of energy propagation, or the ray direction, does not coincide with the direction of the phase velocity, or normal to the phase front. In this case the situation shown in Fig. 1 develops which is the nonlinear analog of optical birefringence. For normal incidence of the laser beam propagating as an ordinary ray, two second-harmonic beams will emerge from the uniaxial crystal slab. The ray corresponding to the wave packet of homogeneous solutions makes an angle ρ inside the crystal with the driven solution of the inhomogeneous wave equations. It should be noted that the harmonic source polarization in the crystal is spatially confined to the region of latter, which coincides with the laser beam.

This "walk-off" or "aperture" effect was noted early in the development of nonlinear optics and shows some similarity with the spatial separation of the homogeneous and inhomogeneous solutions in a cubic crystal, if the angle of incidence deviates strongly from the normal.[6] The effect was carefully analyzed in great detail by Boyd, Ashkin, Dziedzic, and Kleinman.[3] Their paper, which will henceforth be referred to as BADK, pays particular attention to the case of practical importance,

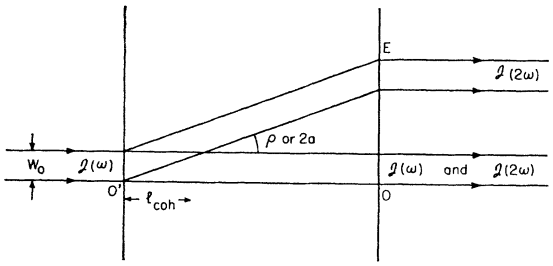

FIG. 1. SH birefringence and internal conical refraction. A laser beam is normally incident on a uniaxial crystal and propagates as an ordinary ray. The SH is polarized in the extraordinary direction. There is a driven SH ray normal to the platelet, while the free SH wave packet gives a ray propagating at an angle ρ inside the crystal. If the coherence length is short, these two harmonic rays have equal intensity. This figure may also be used to describe internal conical refraction in a biaxial crystal, if the SH optic axis OO' is normal to the platelet. The SH intensity propagates along a cone mantle inside the crystal, and emerges as a cylindrical mantle with a base diameter OE.

* Work supported by the Joint Services Electronics Program under Contract No. N00014-67-A-0298-0006.

[1] J. A. Armstrong, N. Bloembergen, J. Ducuing, and P. S. Pershan, Phys. Rev. 127, 1918, (1962).

[2] D. A. Kleinman, Phys. Rev. 128, 1761 (1962).

[3] G. D. Boyd, A. Ashkin, J. M. Dziedzic, and D. A. Kleinman, Phys. Rev. 137, 1305 (1965).

[4] D. A. Kleinman, A. Ashkin, and G. D. Boyd, Phys. Rev. 145, 338 (1966).

[5] M. Born and E. Wolf, *Principles of Optics* (Pergamon Press Inc., New York, 1965), 3rd ed., Chap. XIV.

[6] N. Bloembergen, J. H. Simon, and C. H. Lee, Phys. Rev. 181, 1261 (1969).

in which momentum matching occurs. In this case the laser beam contains the direction, for which $\Delta\mathbf{k}=0$ or l_{coh} becomes infinite. The second-harmonic (SH) field may, of course, still be calculated from the known spatial distribution of the nonlinear source polarization, by introducing the appropriate Green's function. The solutions have been described in detail and have been verified experimentally.[3,4]

The results of BADK are also applicable to biaxial crystals, except when the wave vector $2\mathbf{k}_L$ has a direction in the immediate vicinity of the optical axes. It is the purpose of this paper to extend the analysis of BADK to this special situation.

Intuitively, one may expect the following situation to develop. Because of the frequency dispersion of the optical axes it is possible to propagate a laser beam of finite dimension with a small range of wave vectors $\mathbf{k}_L$, which do not include the direction of the optic axis at the laser frequency, but encompass the optic axis for the second harmonic. The energy propagation of the packet of homogeneous waves containing the direction of the optic axes is known from linear optics to lie on the mantle of a cone.[5] The homogeneous wave solution thus leads to a circular harmonic intensity distribution at the exit face of the biaxial nonlinear crystal plate. Figure 1 may still be used to illustrate this case, if we consider the distance OE as the diameter of a circle. The angle ρ now has a value

$$2a=[(\epsilon_3-\epsilon_2)(\epsilon_2-\epsilon_1)/\epsilon_1\epsilon_3]^{1/2}, \tag{3}$$

where $\epsilon_3>\epsilon_2>\epsilon_1$ are the three principal values of the dielectric tensor at the SH frequency.

In addition to the inhomogeneous solution which is a SH beam coinciding with the laser beam, there will now be a cylindrical mantle of SH intensity coming out of the crystal with a diameter $2aL$, where L is the thickness of the crystal. This result will be confirmed by the Green's function formalism, which will be developed in Sec. II. In Sec. III several details of the application to conical refraction in biaxial crystals are discussed, including the rather special case of exact momentum matching along the optic axis and the effects of misalignment.

The harmonic conical refraction, as depicted in Fig. 1, should be detectable, if a pulsed laser is used with a suitable biaxial crystal of reasonable dimensions. Sufficient harmonic intensity can be generated in a nonphase matched direction. The physical conditions for the observation of a simple ring pattern at the exit face are the following:

(1) The diffraction angle of the primary laser beam should be small compared to the cone apex angle $2a$. For a diffraction limited laser beam of width w_0, this implies $\lambda\ll 2aw_0$.

(2) The angular dispersion between the optic axes at the fundamental and SH frequency should be larger than the diffraction angle.

(3) The thickness of the crystal L should be sufficiently long, to obtain a dark center of the circle, $2aL>w_0$.

(4) The coherence length should be smaller than the length over which the homogeneous and inhomogeneous solutions in Fig. 1 overlap, $l_{\text{coh}}\ll w_0/2a$.

These conditions can be met with a diffraction limited neodymium glass laser beam of diameter $w_0=0.05$ cm in a crystal of α-iodic acid (α-HIO_3), 3 cm long. This orthorhombic crystal belongs to the space group D_2^4-$P_{2_1}P_{2_1}P_{2_1}$ and is piezoelectric with large nonlinear coefficient d_{14} for second-harmonic generation (SHG).[7] It has principal values of index of refraction $n_1=1.8547$, $n_2=1.9829$, $n_3=2.0103$ at $\lambda=0.533\mu$ and $n_1=1.8123$, $n_2=1.9275$, $n_3=1.9508$ at $\lambda=1.065\mu$. In this orthorhombic crystal the direction of the principal axes of the index ellipsoid are, of course, fixed along the orthorhombic axes. One may calculate the direction of the optic axes[5] at these two wavelengths and one finds an angle of 0.8×10^{-2} rad for the frequency dispersion of the direction of the optic axes. The coherence length is estimated from the dispersion in index of refraction along the optic axis to be $l_{\text{coh}}\sim5\ \mu$. The cone aperture is calculated from Eq. (3) to be 6×10^{-2} rad.

For ethylenediamine tartrate (edt), the situations are less favorable, owing to smaller nonlinear coefficient and smaller cone aperture. One has for the index of refraction,[8] $n_1=1.5175$, $n_2=1.6035$, $n_3=1.6095$ at $\lambda=0.45\mu$ and $n_1=1.5010$, $n_2=1.5780$, $n_3=1.5809$ at $\lambda=0.9\mu$, One calculates $2a\cong3\times10^{-2}$ rad, $l_{\text{coh}}\sim9\mu$ and the angular dispersion of the optical axes is of the order of 6×10^{-2} rad.

For Rochelle salt, the numbers are even less favorable.[9] $n_1=1.4991$, $n_2=1.5006$, $n_3=1.5050$ at $\lambda=0.4554\mu$ and $n_1=1.4874$, $n_2=1.4892$, $n_3=1.4928$ at $\lambda=0.649\mu$. One calculates $2a\sim3\times10^{-3}$ rad, $l_{\text{coh}}\sim20\mu$ and the dispersion of the optic axes 7×10^{-2} rad. Although conditions 2–4 may not be met, one should still expect a characteristic intensity pattern which may be calculated by the method described in Secs. II and III. The calculations are valid for an arbitrary thickness L and the case of infinite coherence length is also considered.

When the incident laser beam propagates along the direction of the optic axis at the fundamental frequency, the fundamental light will be refracted into cone mantle, and so will the resulting nonlinear polarization. In this case, the forced solution of the inhomogeneous SH wave equation will be spread into an overlapping cone, while now the homogeneous solution gives rise to a single direction for each direction of polarization. When the

[7] S. K. Kintz, T. T. Perry, and J. G. Bergman, J. Appl. Phys. Letters **12**, 186, (1968).

[8] W. P. Mason, *Piezoelectric Crystals* (Van Nostrand, Inc., New York, 1950); G. D. Boyd (private communication).

[9] Landolt-Bornstein, in *Zahlenwerte and Funktioneu*, edited by K. H. Hellwege and A. M. Hellwege (Springer-Verlag, Berlin, 1959), Vol. II, 6, p. 414–422; (Springer-Verlag, Berlin, 1962), Vol. II, 8.

solid angle of the incident laser beam includes the optic axes, both at the fundamental and the harmonic frequency, a superposition of two cone patterns will result. Thus the case of insufficient angular dispersion may also be included. Although the conditions on optical anisotropy, size, and optical quality of the biaxial crystal are rather stringent, there appears to be little doubt that experimental demonstration of the effect is possible. For this reason and for the sake of completeness, the detailed theory of BADK of parametric generation of light in anisotropic crystals is extended to the special situation of propagation along an optic axis in a biaxial crystal.

II. GREEN'S FUNCTION FOR SH FIELD

The procedure used in this section is the same as that employed in Sec. 5 of BADK. For simplicity the equations will only be given for nonabsorbing crystals, although a weak linear absorption could readily be incorporated in the same way as in BADK.

Expand the nonlinear polarization into a Fourier series.

$$\mathbf{P}^{\mathrm{NL}}(\mathbf{r})=\frac{1}{2\pi}\int \mathbf{P}_{\mathbf{K}}e^{(i\mathbf{K}\cdot\mathbf{r})}d\mathbf{K}. \tag{4}$$

Each component $\mathbf{P}_{\mathbf{K}}$ gives rise to a solution of the field which obeys the inhomogeneous wave equation.

$$\nabla\times\nabla\times\mathbf{E}-(2\omega/c)^2\boldsymbol{\varepsilon}_2\cdot\mathbf{E}=4\pi(2\omega/c)^2\mathbf{P}^{\mathrm{NL}}(\mathbf{r}). \tag{5}$$

One finds, for one polarization mode,

$$\mathbf{E}_{\mathbf{K}}=\frac{4\pi\omega}{nc}\frac{1}{\Delta k}[1-\exp(-i\Delta\mathbf{k}\cdot\hat{z})](\boldsymbol{\gamma}\cdot\mathbf{P}_{\mathbf{K}}^{\mathrm{NL}})e^{i\mathbf{K}\cdot\mathbf{r}}. \tag{6}$$

This is the same form as Eq. (2). Here $\Delta\mathbf{k}$ is given by Eq. (1), and the dyadic $\boldsymbol{\gamma}$ is given by

$$\boldsymbol{\gamma}=\hat{e}\hat{e}\cdot\{[K^2\mathbf{1}-\mathbf{KK}-(2\omega/c)^2\boldsymbol{\varepsilon}_2]^{-1}(K^2-k^2)\}. \tag{7}$$

It represents the projection operator for the nonlinear polarization component which is effective in producing the SH growth, $\hat{e}$ is the unit vector denoting the direction of polarization of the electric field. The term in curly brackets may, near normal incidence, be replaced by unity for the nearly isotropic case. If the inverse Fourier transform of Eq. (6) is taken one finds

$$\mathbf{E}(\mathbf{r})=\frac{1}{2\pi}\int \mathbf{E}_{\mathbf{K}}\exp(+i\mathbf{K}\cdot\mathbf{r})d\mathbf{K}=\int d\mathbf{r}'G(\mathbf{r},\mathbf{r}')\mathbf{P}^{\mathrm{NL}}(\mathbf{r}'), \tag{8}$$

where we have introduced the Green's function $G(\mathbf{r},\mathbf{r}')$.

In the parallel beam approximation the SH polarization has the same transverse spatial distribution in each cross section $0<z'<L$ of the crystal. Assume a linear polarization in the direction $\hat{e}_2$

$$\mathbf{P}^{\mathrm{NL}}(\mathbf{r})=\exp(iK_z z)P(\mathbf{r}_1)\hat{e}_2. \tag{9}$$

Here K_z is twice the z component of the wave vector of the laser beam. The transverse distribution maybe written as the Fourier transform

$$P(\mathbf{r}_1)=\frac{1}{2\pi}\int d\mathbf{K}_1\exp(i\mathbf{K}_1\cdot\mathbf{r})P(\mathbf{K}_1). \tag{10}$$

The Green's function in the parallel beam approximation may from Eqs. (4–8) be expressed as

$$\mathbf{G}(\mathbf{r},\mathbf{r}')=\frac{1}{2\pi}\int d\mathbf{K}_1\sum_{\lambda=1,2}\hat{e}_\lambda\hat{e}_\lambda(2\omega/c)^2(1/k_z^\lambda)i \times\exp[i\mathbf{K}_1\cdot(\mathbf{r}-\mathbf{r}')+ik_z^\lambda(z-z')], \tag{11}$$

where the summation λ is over the two modes of polarization in the crystal, $\hat{e}_\lambda$ is the direction of the λ polarization and k_z^λ is the z component of the wave vector for the SH-field component with polarization λ. This result (11) is valid for any medium, isotropic, uniaxial or biaxial, and the combination of Eqs. (7), (8), and (10), gives the harmonic field anywhere inside the medium. In particular, the field at the exit face is obtained by substituting $z=L$. The approximations that have been made to obtain the simple result (11) are the parallel beam approximation, ignoring the reflected harmonic intensity and taking the magnitude of γ as unity for near normal incidence and small anisotropy.

Let us first apply this formalism to the birefringence in a uniaxial crystal as shown in Fig. 1. The discussion of BADK shows that we may take in the case of extraordinary polarized harmonic field

$$k_z^\lambda=k_e^{(2\omega)}-\rho K_x. \tag{12}$$

The Green's function for this case becomes

$$\begin{aligned}G_e(\mathbf{r}-\mathbf{r}')&\cong\frac{1}{2\pi}\int dK_x dK_y\hat{e}_e\hat{e}_e\left(\frac{2\omega}{c}\right)^2\frac{1}{k_e^{(2\omega)}}i\\ &\times\exp[ik_e^{(2\omega)}(z-z')+ik_y(y-y')\\ &\quad+ik_x(x-x'-\rho z+\rho z')]\\ &=\hat{e}_e\hat{e}_e i\left(\frac{2\omega}{c}\right)^2\frac{2\pi}{k_e^{(2\omega)}}\exp[ik_e^{(2\omega)}(z-z')]\\ &\times\delta(y-y')\delta[(x-x')-\rho(z-z')],\end{aligned} \tag{13}$$

where $\hat{e}_e$ is the direction of the polarization for the extraordinary ray.

In the limit of phase matching $\Delta k=K_z-k_e^{(2\omega)}=0$, the SH fields observed at the exit plane of the crystal is

simply

$$\mathbf{E}_e(x,y,L)=\int_0^L dz'\int dx'dy'\mathbf{G}_e(L-z',x-x',y-y')\times\mathbf{P}^{\mathrm{NL}}(x',y')\exp(iK_z z')$$
$$\cong\hat{e}_e i4\pi\frac{(2\omega)^2}{c^2}\frac{1}{2k_e^{(2\omega)}}\exp(ik_e^{2\omega}L)\times\int_0^L dz'\hat{e}_e\cdot\hat{e}_2 P[x-\rho(L-z'),y] \quad (14)$$

which agrees with Eq. (5.51) of BADK, who concentrated their discussion on the phase-matched case.

In the limit of large phase mismatch, however, the middle of the column is essentially "dark" and it is degenerated into just two spots of dimensions w_0. This can be seen as follows: With the phase-mismatch parameter Δk included, Eq. (14) becomes

$$\mathbf{E}_e(x,y,L)\cong\hat{e}_e i4\pi\frac{(2\omega)^2}{c^2}\frac{1}{2k_e^{(2\omega)}}\exp(ik_e^{(2\omega)}L)\times\int_0^L dz'\hat{e}_e\cdot\mathbf{P}^{\mathrm{NL}}[x-\rho(L-z'),y]e^{i\Delta kz'}$$
$$=\hat{e}_e i4\pi\frac{(2\omega)^2}{c^2}\frac{1}{2k_e^{(2\omega)}}\exp(ik_e^{(2\omega)}L)\times\int\frac{d\mathbf{K}_\perp}{2\pi}(\hat{e}_e\cdot\hat{e}_2)P(\mathbf{K}_\perp)e^{i\mathbf{K}_\perp\mathbf{r}}\times\int_0^L dz'\exp\{i[\Delta kz'-K_x\rho(L-z')]\}. \quad (15)$$

Carrying out first the z' integration, we have

$$\mathbf{E}_e(x,y,L)\cong\hat{e}_e 4\pi\frac{(2\omega)^2}{c^2}\frac{1}{2k_e^{(2\omega)}}\left\{e^{iK_zL}\int\frac{d\mathbf{K}_\perp}{2\pi}(\hat{e}_e\cdot\hat{e}_2)\times\frac{P(\mathbf{K}_\perp)}{\Delta k+K_x\rho}e^{i\mathbf{K}_\perp\mathbf{r}}-\exp(ik_e^{(2\omega)}L)\int\frac{d\mathbf{K}_\perp}{2\pi}(\hat{e}_e\cdot\hat{e}_2)\times\frac{P(\mathbf{K}_\perp)}{\Delta k+K_x\rho}e^{iK_yy}e^{iK_x(x-\rho L)}\right\}. \quad (16)$$

If we have sufficient phase mismatch so that $\Delta k\gg\rho/w_0$ or $\rho l_{\mathrm{coh}}\ll 2\pi w_0$, then the term $K_x\rho$ may be neglected in the denominator of the above integral. We thus have

$$\mathbf{E}_e(x,y,L)\cong\hat{e}_e 4\pi\frac{(2\omega)^2}{c^2}\frac{1}{2k_e^{(2\omega)}}\frac{1}{\Delta k}\times\{e^{iK_zL}\hat{e}_e\cdot\mathbf{P}^{\mathrm{NL}}(x,y)-e^{ik_e^{(2\omega)}L}\hat{e}_2\cdot\mathbf{P}^{\mathrm{NL}}(x-\rho L,y)\}. \quad (17)$$

Since $P^{\mathrm{NL}}(x,y)$ vanishes for $x^2+y^2\gg w_0^2$, this result may be interpreted as follows. The SH intensity consists of two beams. One propagates in the same way as the parallel fundamental beam along the z axis, the other propagates in the x-z plane and makes an angle ρ with the z axis. Both beams have equal intensity and the same transverse intensity distribution. This solution thus confirms the physical reasoning in the introduction which led to the situation shown in Fig. 1.

Turning now to the case of propagation along the optic axis in a biaxial crystal, the geometrical relationship given by Eq. (12) is no longer valid. Describe a wave vector $\mathbf{k}$ in the neighborhood of the direction of the optical axis by its deviation from $\mathbf{k}_{\mathrm{op}}=2\omega c^{-1}\epsilon_2^{1/2}\hat{z}$, namely, by $\mathbf{K}_\perp$ and δk_z as defined in Fig. 2 and Eq. (18). It is characteristic of a medium that the transverse part $K_\perp$ is sufficient to specify the total wave vector $\mathbf{k}_\lambda$. In addition, it also determines the direction of polarization $\hat{e}_\lambda$. Reference 5 may be followed and a detailed geometrical derivation is given in the Appendix. One finds that instead of the geometrical relation Eq. (12), we may now express k_λ to first order in $K_\perp$ as follows:

$$\mathbf{k}_\lambda=\mathbf{K}_\perp+\hat{z}k_z^\lambda,$$
$$k_z^\lambda\cong k_2-ak'[\cos\Omega_k-(-1)^\lambda], \quad (18)$$

where

$$k_2=(2\omega/c)(\epsilon_2)^{1/2},$$
$$a=\tfrac{1}{2}[(\epsilon_3-\epsilon_2)(\epsilon_2-\epsilon_1)/\epsilon_1\epsilon_3]^{1/2}.$$

Here $\epsilon_3>\epsilon_2>\epsilon_1$ are the principal values of the dielectric constants at the SH frequency 2ω. The polarization $\hat{e}_\lambda$ is, to 0th order in $K_\perp/k_2$, given by

$$\hat{e}_\lambda\cong\hat{x}\cos\Omega_\lambda+\hat{y}\sin\Omega_\lambda \quad (19)$$

with

$$\Omega_\lambda=\tfrac{1}{2}\Omega_k'+\tfrac{1}{2}(\lambda-1)\pi.$$

It has been assumed that the optic axis is in the normal or $\hat{z}$ direction. The $\hat{y}$ direction is taken parallel to the medium principal axis, along which the dielectric constant is, ϵ_2 and $\hat{x}=\hat{z}\times\hat{y}$.

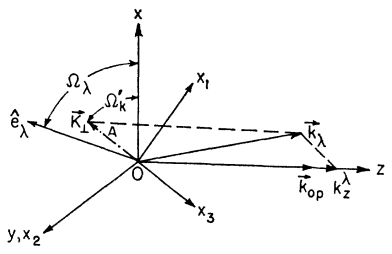

FIG. 2. $\hat{x}_1$, $\hat{x}_2$, and $\hat{x}_3$ are the set of three principal axes of the dielectric tensor such that the dielectric constants satisfy the condition $\epsilon_1<\epsilon_2<\epsilon_3$. x, y, and z form a set of orthogonal axes with y axis antiparallel to $\hat{x}_2$ and with z axis parallel to the optical axis (which lies in the x_1-x_3 plane). It is also normal to the crystal boundary. OA is the projection of the wave vector $\mathbf{k}_\lambda$ onto the x-y plane, and specifies $\vec{K}_\perp$. $\hat{e}_\lambda$ is the polarization vector (which lies in the x-y plane).

The Green's function Eq. (11) now becomes with Eqs. (18) and (19)

$$\mathbf{G}(\mathbf{r},\mathbf{r}')\cong(2\pi)^{-1}e^{ik_2(z-z')}$$
$$\times\sum_\lambda\int k'dk'\int d\Omega_k'(2\pi)^{-1}(\hat{x}\cos\Omega_\lambda+\hat{y}\sin\Omega_\lambda)^2$$
$$\times i4\pi\frac{(2\omega)^2}{c^2}(2k_2)^{-1}\exp\{ik'R\cos(\Omega_\perp-\Omega_k')$$
$$-ika[\cos\Omega_k'-(-1)^\lambda](z-z')\},\quad(20)$$

where

$$R=|\mathbf{r}_\perp-\mathbf{r}_\perp'|,$$
$$\Omega_\perp=\cos^{-1}[(\mathbf{r}_\perp-\mathbf{r}_\perp')\cdot\hat{x}/R],$$

and the square of the vector is the dyadic (outer) product.

The substitution of the first-order approximation for k_z^λ as given by Eq. (18) is valid only if the observation plane is close enough to the source point so that

$$(z-z')/2k_2\ll w_0^2,$$

where w_0 is the effective beam width. Note that this condition restricts us to the region where beam diffraction is negligible, and is equivalent with the near-field criterion for parallel beam approximation.[3] With Eqs. (4), (8), and (20) the harmonic field at the exit face of a biaxial crystal platelet, with the optic axis in the normal direction, can be written

$$\mathbf{E}(x,y,L)=\sum_\lambda\int d\mathbf{K}_\perp(2\pi)^{-1}e^{i\mathbf{K}_\perp\cdot\mathbf{r}}P(\mathbf{K}_\perp)i\left(\frac{2\omega}{c}\right)^2\frac{1}{k_z^\lambda}$$
$$\times\hat{e}_\lambda(\hat{e}_\lambda\cdot\hat{e}_2)\int_0^L dz'\exp(iK_z z')\exp\{ik_z^\lambda(L-z')$$
$$-iak'[\cos\Omega_k'-(-1)^\lambda](L-z')\}.\quad(21)$$

In Sec. III we shall discuss the detailed directional and polarization properties of this field and show that it indeed corresponds to a conical refraction.

III. HARMONIC CONICAL RADIATION

The Green's function given by Eq. (20) implies that the SH field from each slab of harmonic polarization dz is radiated into a cone. If the harmonic polarization is linearly polarized in the direction $\hat{e}_2$, then the contributions to the normal modes, modes $\lambda=1,2$, are complex conjugates, as follows from Eqs. (18)–(20),

$$\mathbf{G}(\mathbf{r},\mathbf{r}')\cdot\hat{e}_2=i\left(\frac{2\omega}{c}\right)^2k_2^{-1}e^{ik_2(z-z')}\int_0^{2\pi}d\Omega_k'(2\pi)^{-1}$$
$$\times(\hat{x}\cos\tfrac{1}{2}\Omega_k'+\hat{y}\sin\tfrac{1}{2}\Omega_k')\cos(\tfrac{1}{2}\Omega_k'-\Phi)$$
$$\times\int_0^\infty k'dk'(e^{ik'\eta}+e^{-ik'\eta}),\quad(22)$$

where

$$\eta=R\cos(\Omega_k'-\Omega)-D(\cos\Omega_k'+1),$$
$$D=a(z-z'),$$
$$\Phi=\cos^{-1}(\hat{x}\cdot\hat{e}_2).$$

To emphasize essential directional effects, the following integral, which ignores the polarization features and the factors in front of the integral of Eq. (22), is considered first:

$$g_0=(2\pi)^{-1}\int_0^{2\pi}d\Omega_k'\int_0^\infty k'dk'e^{ik'\eta}.\quad(23)$$

Integration over k' gives

$$g_0=\int_0^{2\pi}d\Omega_k'(2\pi)^{-1}\frac{\partial}{\partial\eta}\left[\mathrm{PP}\frac{1}{\eta}-i\pi\delta(\eta)\right]+\text{c.c.}\quad(24)$$
$$=\lim_{\epsilon\to+0}(2\pi i)^{-1}\int d\Omega_k'(i)^{-1}[(\eta+i\epsilon)^{-2}+(\eta-i\epsilon)^{-2}],$$

where PP means the Cauchy principal part. We have used the well-known identities

$$\int_0^\infty dke^{ikx}=\pi\delta(x)+i\mathrm{PP}(1/x)$$
$$\lim_{\epsilon\to+0}(x-x_0\pm i\epsilon)^{-1}=\mathrm{PP}(x-x_0)^{-1}\mp i\pi\delta(x-x_0)\quad(25)$$

in the above derivation.

Let us fix z, z' and consider the pattern of g_0 in the $z-z'=d$ plane. The functional form of the integrand in Eq. (24) implies that essential contributions to g_0 are from $\eta=0$. According to the definition of η in Eq. (22), this corresponds, in the $z-z'=d$ plane, to a straight line which makes an angle $(\frac{1}{2}\pi-\Omega_k')$ with the x axis as shown in Fig. 3. As Ω_k' is varied from 0 to 2π, the tip A traces out a locus $OA=\rho'=D(\cos\Omega_k'-1)$. As we add their contributions together, corresponding to the Ω_k' integration, it is clear that they reinforce each other

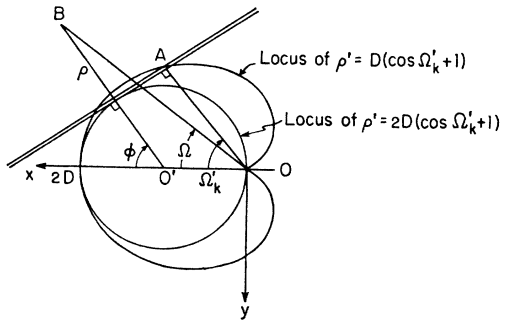

FIG. 3. Schematic diagram for geometrical features of the g_0 integral, given by Eq. (23). The locus $\rho'=D(\cos\Omega_k'+1)$ is the envelope of the circle $\rho'=2D\cos\Omega_k'$ (ρ' measures the distance from the origin O. Ω_k' is the angle between the x axis and the radius vector). B denotes the projection $\mathbf{R}_\perp$ of the point $\mathbf{R}$ in the transverse plane $OB=R$ and $O'B=\rho$.

only in the region described by the envelope of this locus. This envelope is easily shown to be a circle of radius $2D$, with its center lying along x direction and a distance D away from the z axis as shown also in Fig. 3. Therefore, g_0 gives a field pattern which is a cone whose intersection with the transverse plane is a circle as just described. Its radius is proportional to its longitudinal distance $z-z'$ from the radiative source. It is clear from the conservation of power flux that g_0 is inversely proportional to $z-z'$.

Let us define ρ,φ as the coordinates with respect to the center of the circle O' instead of O as shown in Fig. 3. It may be shown that g_0 is independent of the angular variable φ and we may therefore write

$$g_0=[1/(z-z')]g_0'(\rho). \tag{26}$$

To include the polarization effects, Eq. (22) is now integrated to give

$$\mathbf{G}\cdot\hat{e}_2=i(2\omega/c)^2k_2^{-1}e^{ik_2(z-z')}\times\int_0^{2\pi}d\Omega_k'(2\pi)^{-1}(\hat{x}\cos\tfrac{1}{2}\Omega_k'+\hat{y}\sin\tfrac{1}{2}\Omega_k')\times\cos(\tfrac{1}{2}\Omega_k'-\Phi)2\left[\frac{\partial}{\partial\eta}\mathrm{PP}\frac{1}{\eta}\right]. \tag{27}$$

We next apply arguments similar to that used in the paragraph following Eq. (25). There is, however, one modification, that the straight lines considered previously are not of equal magnitude but have an angular dependence on Ω_k' namely, $\cos(\Phi-\frac{1}{2}\Omega_k')$. This same dependence is still valid in the final result with Ω_k' replaced by φ for the "conical circle" of the radiation in the z plane. This is obvious from the way by which the circle is constructed.
Therefore,

$$\mathbf{G}\cdot\hat{e}_2=i(2\omega/c)^2(1/k_2)e^{ik_2(z-z')}(\hat{x}\cos\tfrac{1}{2}\varphi+\hat{y}\sin\tfrac{1}{2}\varphi)\times\cos(\tfrac{1}{2}\varphi-\Phi)g_0'(\rho)/(z-z'). \tag{28}$$

Note that its amplitude

$$|\mathbf{G}\cdot\hat{e}_2|=(2\omega/c)^2k_2^{-1}|\cos(\tfrac{1}{2}\varphi-\Phi)|\,|g_0(\rho)|/|z-z'| \tag{29}$$

has an angular dependence of $\cos(\Phi-\frac{1}{2}\varphi)$ around the circle in the transverse plane for the case of linear polarization.

A. Conical Refraction for Harmonic Generation with Momentum Mismatch

Usually the direction of the optic axis will not correspond to a direction of momentum matching. We must add the radiation fields of each slab dz with the appropriate phase. If $\Delta k=K_z-k_z^{\lambda}$ denotes the mismatch, integration of Eq. (20) over z' yields the SH field

$$\mathbf{E}(x,y,L)\cong\frac{(2\omega)^2}{c^2}(1/k_2)\sum_{\lambda=1,2}\int dK_1(2\pi)^{-1}e^{i\mathbf{K}_1\cdot\mathbf{r}}P(K_1)\times\{\Delta k+ak'[\cos\Omega_k'-(-1)^{\lambda}]\}^{-1}\hat{e}_{\lambda}(\hat{e}_{\lambda}\cdot\hat{e}_2)\times[e^{iK_zL}-\exp\{k_2-ak'[\cos\Omega_k'-(-1)^{\lambda}]\}L]. \tag{30}$$

For $\Delta k\gg 2a/w_0$, where w_0 is a characteristic transverse dimension of the beam, the following approximation is valid:

$$\mathbf{E}(x,y,L)\cong\left(\frac{2\omega}{c}\right)^2\frac{1}{k_2\Delta k}\Big\{\hat{e}_2P(x,y)e^{iK_zL}-e^{ik_2L}\int d\Omega_k'(2\pi)^{-1}P(k',\Omega_k')(\hat{x}\cos\tfrac{1}{2}\Omega_k'+\hat{y}\sin\tfrac{1}{2}\Omega_k')\times\cos(\tfrac{1}{2}\Omega_k'-\Phi)\int_0^{\infty}k'dk'[e^{ik'\eta'}+e^{-ik'\eta'}]\Big\}, \tag{31}$$

where

$$\eta'=r_1\cos(\Omega-\Omega_k')-aL(\cos\Omega_k'+1).$$

The first term represents a beam which propagates in the same way as the fundamental beam along the z axis. In other words, it has the same phase velocity $2\omega/k$ as the fundamental beam, and the same cross-sectional distribution as the polarization. The second term represents a beam of entirely different characteristics. It may be written in a little different form, by inversely fourier transforming $P(K_1)$ to $P(r_1)$ as

$$\mathbf{E}(x,y,L)=-\left(\frac{2\omega}{c}\right)^2(k_2\Delta k)^{-1}e^{ik_2L}\times\int dr_1'(2\pi)^{-1}P(r_1')\mathbf{G}'(r_1-r_1',L)\cdot\hat{e}_2, \tag{32}$$

where

$$\mathbf{G}'(r_1-r_1',L)=\int\frac{d\Omega_k'}{2\pi}(\hat{x}\cos\tfrac{1}{2}\Omega_k'+\hat{y}\sin\tfrac{1}{2}\Omega_k')\cos(\tfrac{1}{2}\Omega_k'-\Phi)\times\int_0^{\infty}k'dk'(e^{ik'\eta''}+e^{-ik'\eta''}),$$

$$\eta''=R\cos(\Omega-\Omega_k')-aL(\cos\Omega_k'+1).$$

$\mathbf{G}'$ is recognized as a special form of the Green's function $\mathbf{G}$ with $z'=0$, as given by Eqs. (24) and (28). The implication of the above form is then very clear. It represents a conical pattern, starting from the plane of entry. If the crystal is thick enough, $2aL\gg w_0$, the SH intensity at the exit face will be in the pattern of a ring with diameter $2aL$ and width w_0. The polarization and intensity distribution around the ring is given by Eq. (28). This confirms the heuristic argument of the

introduction. It is the nonlinear analog of internal conical refraction.

B. Phase-Matched Case

For $\Delta k=0$, the z' integration of Eq. (22) leads to the harmonic fields,

$$\mathbf{E}(x,y,L)\propto e^{iK_zL}\int_{x-2h}^{x}dx'\int_{y-m}^{y+m}dy'P(x',y')1/(x-x')$$
$$\times[\hat{x}(x-x')+\hat{y}(y-y')][(x-x')\cos\Phi+(y-y')\sin\Phi]$$
$$\times[(x-x')^2+(y-y')^2]^{-1}, \quad (33)$$

where

$$h=aL, \quad m=[(x-x')(2h-x+x')]^{1/2}.$$

This result may be made physically plausible by the following argument. Consider the first contribution due to a source field which is infinitesimally thin in the transverse directions and is of length L in the z direction, i.e., we let

$$\mathbf{P}^{\mathrm{NL}}(\mathbf{r})=\hat{e}_2\delta(x)\delta(y)e^{iK_zz} \quad \text{for} \quad 0<z<L \quad (34)$$
$$=0 \quad \text{elsewhere.}$$

From the discussion of the Green's function at the beginning of this section it follows that each point $(0,0,z')$ radiates into a circle

$$r_\perp/\cos\Omega=(L-z')2a$$

in the exit plane. On this circle, the nonuniformity of the field amplitude around its circumference is given by the factor

$$\hat{r}_\perp\cdot\hat{e}_2=[x\cos\Phi+y\sin\Phi]/(x^2+y^2)^{1/2},$$

whereas the vector character of the field is indicated by

$$\hat{r}_\perp=\hat{x}x+\hat{y}y.$$

The dependence on z is clear; the field amplitude is proportional to $(L-z')^{-1}$ or $2a\cos\Omega/r_\perp$, and the phase is determined by the factor

$$e^{ik_2(L-z')}=\exp\{ik_2r_\perp/[2a\cos\Omega]\}.$$

As we move the radiating element away from the exit plane, with the value of z' decreasing from L to 0, the diameter of the circle increases from 0 to $2aL$. It is clear then that total contribution to the SH field due to the line source is

$$d\mathbf{E}\propto 0 \quad \text{for} \quad r_\perp/\cos\Omega>2aL$$
$$\propto 1/x(\hat{x}x+\hat{y}y)(x\cos\Phi+y\sin\Phi)/(x^2+y^2) \quad \text{for} \quad r_\perp/\cos\Omega<2aL. \quad (35)$$

Note that we have the dependence of $1/x$ here rather than $L-z'$ or $2a\cos\Omega/r_\perp$. This is because the circles in the exit plane are clustered closer and closer together as we move away from the x axis in the increasing Ω direction. The density of such clustered circle lines can easily be shown to be proportional to $(\cos\Omega)^{-2}$. It is then multiplied by $2a\cos\Omega/r_\perp$ to give $2a/x$ as the resultant dependance. When the integration of Eq. (31) over a transverse cross section is carried out, Eq. (33) is recovered.

For a Gaussian transverse distribution and a thick crystal, $L\gg w_0/2a$, Eq. (33) reduces, in the region $x\gg w_0$, to

$$\mathbf{E}(x,y,L)\propto\hat{r}_\perp\cos(\Phi-\Omega)\int_{x-2h}^{x}dx'\int_{y-m}^{x+m}dy'$$
$$\times\frac{1}{x-x'}e^{-4(x'^2+y'^2)/w_0^2}$$
$$=\frac{\sqrt{\pi}}{2}\hat{r}_\perp\cos(\Phi-\Omega)\int_{x-2h}^{x}dx'\frac{e^{-4x'^2/w_0^2}}{x-x'}$$
$$\times\left\{\mathrm{erf}\left(\frac{y+m}{\frac{1}{2}w_0}\right)-\mathrm{erf}\left(\frac{y-m}{\frac{1}{2}w_0}\right)\right\}.$$

Inside the circle $(x-h)^2+y^2\leq h^2$ and away from its circumference so that the region which is a distance of the order of w_0 away from it is excluded, $\mathbf{E}$ is further reduced to

$$\mathbf{E}(x,y,L)\propto\hat{r}_\perp\cos(\Phi-\Omega)\int_{-\infty}^{\infty}dx'\frac{1}{x-x'}e^{-4x'^2/w_0^2}$$
$$\times\int_{-\infty}^{\infty}dy'e^{-4y'^2/w_0^2} \quad (36)$$
$$\cong\hat{r}_\perp[\tfrac{1}{2}(\sqrt{\pi})w_0]^2\cos(\Phi-\Omega)/x$$

Note that its amplitude would have been proportional to $1/x$ and independent of y if the beam is unpolarized. Effect of the linear polarization, on the other hand, gives rise to the factor $\cos(\Phi-\Omega)$. This implies that we could observe a dark line at the angle $\Omega=\Phi-\frac{1}{2}\pi$ for the linearly polarized laser input.

Near the circumference, $(x,h)^2+y^2\sim h^2$, we have instead

$$\mathbf{E}(x,y,L)\propto\hat{r}_\perp(\tfrac{1}{2}\sqrt{\pi})\frac{\cos(\Phi-\Omega)}{x}\int_{x-2h}^{x}dx'e^{-4x'^2/w_0^2}$$
$$\times\int_{y-m}^{\infty}dy'e^{-4y'^2/w_0^2}$$
$$\cong\hat{r}_\perp(\tfrac{1}{2}\sqrt{\pi})\frac{\cos(\Phi-\Omega)}{x}\left\{(\tfrac{1}{2}w_0^2)\pi\right.$$
$$-\tfrac{1}{2}w_0\sqrt{\pi}\,\mathrm{erf}\left(\frac{x-2h}{\frac{1}{2}w_0}\right)-\int_{x-2h}^{\infty}dx'e^{-4x'^2/w_0^2}$$
$$\left.\times\mathrm{erf}\left(\frac{y-[x(2h-x)+xx']^{1/2}}{\frac{1}{2}w_0}\right)\right\}. \quad (37)$$

It falls off nearly as an error function of width w_0 as the observation point (x,y) is moved out of the circle, but one may expect some intensity everywhere inside the circle in the phase-matched case.

C. Effect of Misalignment

The preceding results are valid for a parallel source beam directed exactly along the optical axis. As we have already mentioned, the optical axis corresponds to a singular point $\mathbf{k}_{op}$ in the $\mathbf{k}$ space so that physical results depend critically upon the specific form of the source $\mathbf{P}^{NL}$. We expect that essential changes in the results will occur even if there is only a small amount of misalignment off the optical axis. In the case of large misalignment, i.e., when the optic axis is not contained in the bundle of k directions of the incident beam, one should, of course, revert to the case of optical birefringence. The polarization should also vary drastically during the transition from the aligned to the misaligned case. These effects will now be analyzed somewhat more quantitatively.

Let us consider the normal incidence of fundament a laser beam on a biaxial crystal plate. Assume that the resulting nonlinear polarization for SHG is a parallel beam of the form given by Eq. (9). While z still denotes the normal to the plate, it no longer coincides with the optical axis $\hat{k}_{op}$ corresponding to misalignment. We shall use the angular parameters θ_d and α to specify uniquely the z direction with respect to the set of crystal fixed axes x_1, x_2, x_3. Here θ_d denotes the angle between $\hat{z}$ and the optical axis, while α is the angle subtended by the x_1-x_3 plane and the z-$\hat{k}_{op}$ plane. Or

$$\theta_d \equiv \cos^{-1}\hat{z}\cdot\hat{k}_{op},$$
$$\alpha \equiv \cos^{-1}[\hat{x}_2\cdot(\hat{z}\times\hat{k}_{op})/|\hat{z}\times\hat{k}_{op}|].$$

In the limit of small misalignment $\theta_d \ll 1$, it is straightforward to show from Eqs. (18) and (19) that k_λ' and $\hat{e}_\lambda'$ may be expressed in terms of θ_d and α as

$$\mathbf{k}_\lambda' = \mathbf{K} + \hat{z}\{k_2 - \theta_d(K_x\cos\alpha + K_y\sin\alpha) - a[\cos(\Omega_k'+\alpha)-(-1)^\lambda] \times[k'^2 + 2\theta_d k_2 k'\cos(\alpha+\Omega_k') + (\theta_d k_2)^2]^{1/2}\} \quad (18')$$

with

$$\Omega_k' = \cos^{-1}(\mathbf{K}_\perp\cdot\hat{x})$$

and

$$k' = |\mathbf{K}_\perp|,$$

and

$$\hat{e}_\lambda' \cong \hat{x}\cos[\tfrac{1}{2}(\Omega_k'-\alpha)+\tfrac{1}{2}(\lambda-1)\pi] + \hat{y}\sin[\tfrac{1}{2}\Omega_k'-\alpha)+\tfrac{1}{2}(\lambda-1)\pi]. \quad (19')$$

The Green's function may therefore be written

$$\mathbf{G}(\mathbf{r},\mathbf{r}') \cong i\left(\frac{2\omega}{c}\right)^2 (k_2)^{-1} e^{ik_2(z-z')} \times \sum_{\lambda=1,2} (2\pi)^{-1}\int d\mathbf{K}_\perp \hat{e}_\lambda'\hat{e}_\lambda' \exp\{i\mathbf{K}_\perp\cdot(\mathbf{r}-\mathbf{r}') - ia(z-z')[\cos(\Omega_{k'}+\alpha)-(-1)^\lambda] \times[k'^2+2k'k_2\theta_d\cos(\Omega_k'+\alpha)+(k_2\theta_d)^2]^{1/2}\}. \quad (20')$$

Consider now the limit when the deviation of the z direction from the optical axis is much smaller than the effective beam spread, i.e., $k_2\theta_d \ll (K_\perp)_{eff}$ where $(K_\perp)_{eff}$ is effective radius of the sphere in $\mathbf{k}$ space over which the above integral is carried out. It is of the same order as the inverse beam width w_0^{-1}. For a source field linearly polarized in the $\hat{e}_2$ direction, we may impose the same conditions and employ the same techniques, which enabled us to reach Eq. (28), to yield

$$\mathbf{G}\cdot\hat{e}_2 \cong i\left(\frac{2\omega}{c}\right)^2 k_2^{-1} e^{ik_2(z-z')}[\hat{x}\cos\tfrac{1}{2}(\varphi-\alpha)+\hat{y}\sin\tfrac{1}{2}(\varphi-\alpha)] \times\cos[\tfrac{1}{2}(\varphi-\alpha)-\Phi](z-z')^{-1}g_0'(\rho)\cos\{a(z-z')k_2\theta_d \times\cos(\varphi+\alpha)[\cos(\varphi+\alpha)-1]\}. \quad (38)$$

Comparison with Eq. (28) shows that the last cosine factor is the essential modification due to the small misalignment of the beam. Therefore, the conical form of the harmonic radiation is still preserved but the angular distribution around the cone is modified.

In the case where the misalignment angle is so large as to be greater than the effective beam spread, i.e., $k_2\theta_d \gg (K_\perp)_{eff}$, we have, instead of Eq. (38),

$$\mathbf{G}(r,r') \cong (2\pi)^{-1}e^{ik_2(z-z')}\sum_\lambda \int d\Omega_k'\hat{e}_\lambda'\hat{e}_\lambda'\frac{1}{k_2} \times\exp\{-ia(z-z')[\cos(\Omega_k'+\alpha)-(-1)^\lambda]k_2\theta_d\} \times\int_0^\infty k'dk' \exp\{ik'R\cos(\Omega_k'-\Omega)-ik'a(z-z') \times[\cos(\Omega_k'+\alpha)-(-1)^\lambda]\cos(\Omega_k'+\alpha)\}. \quad (39)$$

Note that the exponential term preceding the k' integral has a faster varying phase than the term inside the integral. It may thus be replaced by a term f_λ which has the property that

$f_\lambda = 1$ for $|\cos(\Omega_k'+\alpha)-(-1)^\lambda| < [\theta_d k_2 a(z-z')]^{-1} \ll 1$
$= 0$ otherwise.

The k' integral in turn may be approximated by

$$\int_0^\infty k'dk' \exp\{ik'R\cos(\Omega-\Omega_k')-(-1)^\lambda ik'a(z-z') \times[\cos(\Omega_k'+\alpha)-(-1)^\lambda]\},$$

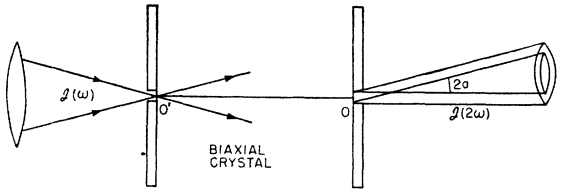

FIG. 4. External conical refraction of SH radiation. The apertures O and O' are so placed that OO' is an optic axis of the biaxial crystal at the SH frequency. The convergent incident lasser beam fills a solid angle containing the direction OO'.

in the region $\Omega_k'+\alpha\approx\lambda\pi$ which is of main interest due to the presence of f_λ. This is of similar form as that of the integral in Eq. (23). It can be evaluated in the similar fashion as previously and the picture of Fig. 3 is once again appropriate here. There is, however, one important modification. That is, that only a small fraction of the locus $\rho=a(z-a')[\cos(\varphi+\alpha)-(-1)^\lambda]$, which corresponds to $\varphi\approx\lambda\pi-\alpha$, will add up coherently. The resultant field pattern in x-y plane will therefore not be a circle as in Fig. 3 but instead just be two points on the circle with φ equal to $\pi-\alpha$ and $-\alpha$, respectively. In other words, double refraction type of SHG instead of conical refraction will result.

IV. CONCLUSION

Detailed calculations confirm the existence of the phenomenon of internal conical refraction in SH generation. It is clear that the same arguments hold for any parametric generation process, e.g., third-harmonic generation, sum or difference frequency mixing when the wave vector of the nonlinear polarization is parallel to the optic axis at the newly generated frequency.

The case that the incident light beam(s) propagate(s) along an optic axis at the incident frequency was mentioned in the Introduction. In this case the nonlinear polarization source is itself spread into a cone mantle. Detailed calculations could again be carried out by the Green's-function technique.

There is also a nonlinear analog to the phenomenon of external conical refraction. In this case the fundamental beam is focused onto a pinhole at the entrance face of the crystal. Harmonic polarization is created with a distribution of transverse $\mathbf{k}$ vectors. A pinhole at the exit face selects the contribution from those Fourier components that give rise to energy propagation along the optic axis defined by the two pinholes. The resulting harmonic radiation at the exit face will emerge in a cone mantle, as shown in Fig. 4.

These effects are accessible to experimental observation, but the polarization effects will be obscured by natural optical activity, which occurs for example in α-iodic acid near the optic axes.

APPENDIX

A proof of Eqs. (18) and (19) is presented here. It is well known that the wave normals $\mathbf{k}_\lambda$ satisfy Fresnel's equations. It has also been shown that the velocity of propagation is given by

$$v_\lambda'^2=(2\omega)^2/(k^\lambda)^2=(1/2)[v_1^2+v_3^2+(v_1^2-v_3^2)\cos(\theta_1-\theta_2)], \quad \text{(A1)}$$

in terms of the angles θ_1 and θ_2 which the wave vector $\mathbf{k}$ makes with the two optical axes as shown in Fig. 5. v_1, v_2, and v_3 denote the principal velocities of propagation with $v_1>v_2>v_3$. They are characteristic of a particular biaxial crystal and are simply related to the dielectric constants ϵ_1, ϵ_2, and ϵ_3 of the three principal dielectric axes by $v_i=c/\sqrt{\epsilon_i}$ with $i=1, 2, 3$. When the wave vectors are close to one of the optical axes, namely, axis OP in Fig. 5, it is apparent that we have $\theta_1\ll1$ and $\theta_2\approx2\beta-\theta_1\cos\Omega_k'$. It is then straightforward to show that Eq. (A1) reduces to

$$v_\lambda'^2\approx v_2^2+\tfrac{1}{2}(v_1^2-v^2{}_3)(\sin2\beta)(\cos\Omega_k'{}_3-(-1)^\lambda\theta_1), \quad \lambda=1,2.$$

This implies, following the relation $v=(2\omega)/k$, that the wave number is

$$k^\lambda=(2\omega)/v_\lambda\approx\frac{(2\omega)}{v_2}\left\{1-\frac{1}{2}\frac{\tfrac{1}{2}(v_1^2-v_3^2)\sin2\beta}{v_2^2}\times[(\cos\Omega_k'+1)]\theta_1\right\}. \quad \text{(A2)}$$

For small transverse component $K_\perp$, however, the longitudinal component k_z^λ will be to first order the same as the wave number. Thus, we conclude, recognizing $k_2=2\omega/v_2=2\omega\sqrt{\epsilon_2}/c$ and $k'\approx k_2\theta_1$ that

$$\mathbf{k}^\lambda=\mathbf{K}_\perp+\hat{z}\{k_2-k'a'[\cos\Omega_k'-(-1)^\lambda]\},$$
$$a'=\tfrac{1}{4}[(v_1^2-v_3^2)/v_2{}^3]\sin2\beta.$$

It is identical with Eq. (18) provided $a'=a$. This can easily be verified by recalling the definition $v_i=c/\sqrt{\epsilon_i}$ and using the relation

$$\tan\beta=[(\epsilon_2/\epsilon_1-1)/(1-\epsilon_2/\epsilon_3)]^{1/2}, \quad \text{(A3)}$$

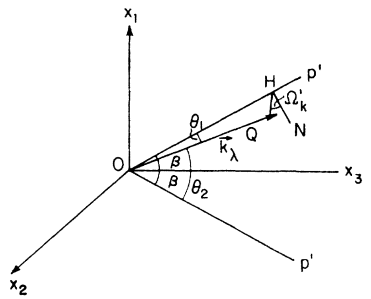

FIG. 5. Diagram showing the geometrical relation of the wave vector $\mathbf{k}_\lambda$ and the optic axes OP and OP'. These lie in the plane normal to $\hat{x}_2$ and make equal angles β with $\hat{x}_3$.

indeed, then

$$a'=\frac{1}{4}\frac{v_1^2-v_3^2}{v_2^2}\sin 2\beta$$
$$=\frac{1}{2}\frac{v_1^2-v_3^2}{v_2^2}\frac{\tan\beta}{(1+\tan^2\beta)}$$
$$=\frac{1}{2}\frac{v_1^2-v_3^2}{v_2^2}\frac{[(v_1^2-v_2^2)(v_2^2-v_3^2)]^{1/2}}{(v_1^2-v_3^2)}$$
$$=a.$$

Equation (A3) determines the angle β between the optical axis and the axis $\hat{x}_3$ in terms of three principal dielectric constants. It can readily be verified.

We now proceed to establish Eq. (19). To find the polarization directions $\hat{d}_\lambda$ of the displacement vectors associated with a given wave propagation direction $\hat{k}$, we employ the geometrical method of ellipsoid.[5] The ellipsoid under consideration is described by

$$x_1^2/\epsilon_1+x_2^2/\epsilon_2+x_3^2/\epsilon_3=1.$$

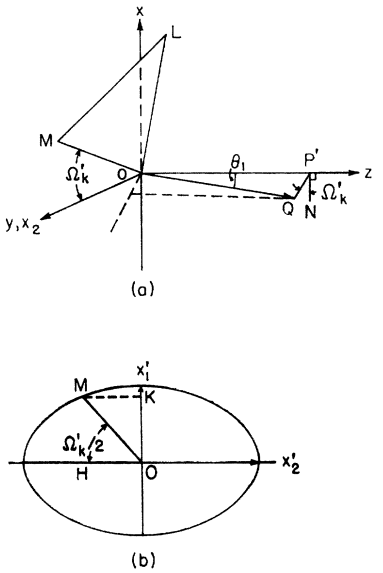

FIG. 6. Diagram for the geometrical construction of the polarization vectors, as explained in the Appendix. The plane OML is normal to the wave vector OQ. The intersection of the wave vector ellipsoid with the plane OML is the ellipse shown in Fig. 6(b).

x_1, x_2, and x_3 are the coordinates along the three principal dielectric axes. We thus draw a plane, passing through the origin (0,0,0) and perpendicular to the direction $\hat{k}$. The intersection of this plane and the ellipsoid is an ellipse, its major and minor axes give the desired directions $\hat{d}_\lambda$. When $\hat{k}$ is along the singular direction of the optical axis, the ellipse degenerates into a circle of radius $\sqrt{\epsilon_2}$. If, however, $\hat{k}$ deviated infinitesinally from $\hat{z}$, the ellipse is described by

$$x_1'^2/\epsilon_1'+x_2'^2/\epsilon_2'=1, \tag{A4}$$

where the major and minor axis ϵ_1', ϵ_2' are given by the Fresnel's equation. Namely,

$$\sqrt{\epsilon_\lambda'}=c/v_\lambda'=ck^\lambda/2\omega=(c/2\omega)\{k_2-ak'[\cos\Omega_k'-(-1)^\lambda]\}$$

x_1', x_2' are orthogonal coordinates linearly related to x_1, x_2, and x_3. To find such relation explicitly, we refer to Fig. 6. The y axis coincides with x_2 axis and $\hat{z}$ is the direction for the optical axis as in Fig. 2. OQ denotes the direction of the $\mathbf{k}$ vector under consideration. Its deviation from $\hat{z}$ is described by parameters θ_1, Ω_k'. The ellipse associated with the vector OP is shown in Fig. 6(b). It lies in the plane MOL in Fig. 6(a). Its intersection with the x-y plane is denoted by OM which is, of course, $\sqrt{\epsilon_2}$ in length. With the knowledge of the length of the ellipse axes $\sqrt{\epsilon_1'}$, $\sqrt{\epsilon_2'}$, and $OM=\sqrt{\epsilon_2}$ we can determine the angle $\angle MOH$. Referring to Fig. 6(b), we can see that OH and OK satisfy the following set of equations:

$$(OH)^2+(OK)^2=\epsilon_2,$$
$$(OH)^2/\epsilon_1'+(OK)^2/\epsilon_2'=1,$$

which have solution

$$OH=c(1-v_1'^2/v_2^2)^{1/2}/(v_2'^2-v_1'^2)^{1/2},$$
$$OK=c(c_2'^2/v_2^2-1)^{1/2}/(v_2'^2-v_1'^2)^{1/2},$$

therefore, using Eq. (A2), we have

$$\angle MOH=\tan^{-1}[(OK)/(OH)]$$
$$=\tan^{-1}[(v_2'-v_2^2)/(v_2^2-v_1'^2)]^{1/2}$$
$$=\tan^{-1}[(1-\cos\Omega_k')/(1+\cos\Omega_k')]$$
$$=\Omega_k'.$$

As θ_1 approaches zero, the plane OML, in which the ellipse lies, tends to coincide with the x-y plane. Therefore, the major axis x_2' which we identify as $\hat{d}_2$, makes and angle $(\Omega_k'-\frac{1}{2}\Omega_k')=\frac{1}{2}\Omega_k'$ with the x axis and minor axis x_1' identified as $\hat{d}_1$, makes an angle $(\frac{1}{2}\Omega_k'+\frac{1}{2}\pi)$ with $\hat{x}$. Eq. (19) then follows immediately.